ISME

Mechanical and Thermal Stresses in a Linear Plastic FGM Hollow Cylinder Due to Axisymmetric Loads

M. Jabbari[*]
Associate Professor

M. Shokouhfar[†]
M.Sc.

A. Hatefkia[‡]
M.Sc.

M. R. Eslami[§]
Professor

In this paper, an analytical solution for computing the linear plastic stresses, critical temperature and pressure in an FGM hollow cylinder under the internal pressure and temperature is developed. It has been assumed that the modulus of elasticity and thermal coefficient of expansion were varying through thickness of the FGM material according to a power law relationship. The Poisson's ratio was considered constant throughout the thickness. The general forms of thermal and mechanical boundary conditions were considered on the inner surface. In the analysis section, the effect of non-homogeneity in FGM cylinder was implemented by choosing a dimensionless parameter, named m, which could be assigned an arbitrary value affecting the stresses in the cylinder. Distribution of stresses in radial and circumferential direction for FGM cylinders under the influence of internal pressure and temperature gradient were obtained. Graphs of critical temperature and pressure versus radius of the cylinder were plotted. Cases of pressure and temperature loadings were considered separately. The direct method has been considered to solve the heat conduction and Navier equations. The outer pressure for all over the cylinder goes to the plastic region when $T_i=T_o=P_i=0$ and by increasing the modules of elasticity the pressure will increase. By substituting M=0 in radial linear plastic stress formula, the perfect plastic equation will yield. By putting $\epsilon_{rr}^{p} = \epsilon_{rr,r}^{p} = 0$ in radial linear plastic stress formula, it turns to the radial elastic stress.

Keywords: Hollow cylinder; non-homogenous; axisymmetric; FGM; Elastic-Plastic Analysis

1 Introduction

Functionally graded material (FGM) is heterogeneous material in which the elastic and thermal properties change from one surface to the other, gradually and continuously. Since ceramic has good heat resistance to corrosion and erosion and metal has high fracture toughness, ceramic-Metal FGM may work at super high-temperatures or under high-temperatures difference and also corrosive fields. In effect, the governing equation of temperature and stress distributions coordinate dependent as the material properties are functions of position.

[*] Associate Professor, Department of Mechanical Engineering, South Tehran Branch, Islamic Azad University, Tehran, Iran Mohsen.jabbari@gmail.com

[†]Corresponding Author, Department of Mechanical Engineering, South Tehran Branch, Islamic Azad University, Tehran, Iran Miladshokouhfar@gmail.com

[‡] Department of Mechanical Engineering, South Tehran Branch, Islamic Azad University, Tehran, Iran Ati.hatefkia@yahoo.com

[§] Professor and Fellow of the Academy of Sciences, Mechanical Engineering, Department of Mechanical Engineering, Amirkabir University of Technology, Tehran, Iran Eslami@aut.ac.ir

There are some analytical thermal and stress calculations for functionally graded material in the on-dimensional case for thick cylinders and spheres [1, 2]. The authors have considered the non-homogeneous material properties as liner function of radius.

M. Jabbari et al. [3] studied a general solution for mechanical and thermal stresses in a functionally graded hollow cylinder due to non-axisymmetric steady-state load. They applied separation of variables and complex Fourier's series to solve the heat conduction and Navier equation. Poultangari et al. [4] presented functionally graded hollow spheres under non-axisymmetric thermo-mechanical loads. Lu yunbing et al. [5] found ceramic/metal functionally gradient material (FGM) has gradient ingredient distribution, so its properties of the heat transfer and thermo elastic mechanics are much better than that of the homogenous materials. In that paper, a model is adopted in which the material ingredients and the material properties in the middle layer change continuously. Shariyat et al. [6] presented nonlinear transient thermal stress and elastic wave propagation analyses of thick temperature-dependent FGM cylinders, using a second-order point-collocation method. In another work [7], he found an algorithm for nonlinear transient behavior analysis of thick functionally graded cylindrical vessels or pipes with temperature-dependent material properties under thermo-mechanical load. Chen and Lim [8] presented elastic mechanical behavior of nano-scaled FGM films incorporating surface energies. X.Y. Li, H.J. Ding, W.Q. Chen[9] considers the bending of transversely isotropic circular plates with elastic compliance coefficients being arbitrary functions of the thickness, subject to a transverse load in the form of the ark (k is zero or a finite even number). Afsar and Sekine [10] presented inverse problems of material distributions for prescribed apparent fracture toughness in FGM coatings around a circular hole in infinite elastic media. Vahid Tajeddini et al. [11] described a study of three-dimensional free vibration analysis of thick circular and annular isotropic and functionally graded (FG) plates with a variable thickness along the radial direction. Asghar Nosier, FamidaFallah [12] based on the first-order shear deformation plate theory with von Karman non-linearity, the non-linear axisymmetric and asymmetric behavior of functionally graded circular plates under transverse mechanical loading are investigated. Zhang and Zhou [13] presented a theoretical analysis of FGM thin plates based on the physical neutral surface. Fazelzadeh and Hosseini [14] presented aero-thermoelastic behavior of supersonic rotating thin-walled beams made of functionally graded materials. Ootao and Tanigawa [15] analysed the transient thermo elastic problem of the functionally graded thick strip due to non-uniform heat supply. They obtained the exact solution for the two-dimensional temperature change in a transient state, and thermal stresses of a simple supported strip under the state of plane strain. Jabbari et al. [16] studied the mechanical and thermal stresses in the functionally graded hollow cylinder due to radial symmetric loads. They assumed the temperature distribution to be a function of radial direction. They applied a direct method to solve the heat conduction and Navier equations. Farid et al. [17] presented three-dimensional temperature-dependent free vibration analysis of functionally graded material curved panels resting on two-parameter elastic foundation using a hybrid semi-analytic, differential quadrature method. Bagri and Eslami [18] presented generalized coupled thermo elasticity of functionally graded annular disk considering the Lord–Shulman theory. Samsam et al. [19] presented buckling of thick functionally graded plates under mechanical and thermal loads. Jabbari et al [20] studied an axisymmetric, mechanical and thermal stresses in a thick short length functionally graded material cylinder. They applied separation of variables and complex Fourier's series to solve the heat conduction and Navier equation.

M. Zamani nejad and G.H. Rahimi [21] Using the infinitesimal theory of elasticity, closed-form solutions for one-dimensional steady-state thermal stresses in a rotating functionally graded (FGM) pressurized thick-walled hollow circular cylinders are obtained under generalized plane strain, and plane stresses assumptions, respectively.

R.C. Batra G.L. Iaccarino [22] found closed-form solutions for axisymmetric plane strain deformations of a functionally graded circular cylinder comprised of an isotropic and incompressible second-order elastic material with module varying only in the radial direction. Cylinder's inner and outer surfaces are loaded by hydrostatic pressures. Three-dimensional thermo-elastic analysis of a functionally graded cylindrical panel with finite length and subjected to non-uniform mechanical and steady-state thermal loads are carried out by Z.S. Shao, T.J. Wang [23]. The adjective "plastic" comes from the classical Greek verb πλάσσειν Meaning "to shape"; it thus describes materials, such as ductile metals, clay, or putty, which have the property that bodies made from them can have their shape easily changed by the application of appropriately directed forces, and retain their new shape upon removal of such forces. The shaping forces must, of course, be of sufficient intensity otherwise. A mere breath could deform the object but often. Such intensity is quite easy to attain, and for the object to have a useful value, it may need to be hardened, for example, through exposure to air or the application of heat, as is done with ceramics and thermosetting polymers. Other materials above all metals are quite hard at ordinary temperatures and may need to be softened by heating in order to be worked. It is generally observed that the considerable deformations which occur in the plastic shaping process are often accompanied by very slight, if any volume changes. Consequently, plastic deformation is primarily a distortion, and of the stresses produced in the interior of the object by the shaping forces applied to the surface, it is their deviators that do most of the work. A direct test of the plasticity of the material could thus be provided by producing a state of simple shearing deformation in a specimen through the application of forces that result in a state of shear stress.

In a soft, semi-fluid material such as clay, or soil in general, this may be accomplished by a direct shear test such as the shear-box test. In hard solids such as metals, the only experiment in which uniform simple shear is produced is the twisting of a thin-walled tube, and this is not always a simple experiment to perform. A much simpler test is the tension test [24].

There are new works of plasticity for FGMs materials. Y.M. Shabana, N. Noda presented thermo-elasto-plastic stresses in functionally graded materials subjected to be thermal loading taking residual stresses of the fabrication process into consideration [25]. A. N. Eraslan & T. Akis presented plane strain analytical solutions for a functionally graded elastic–plastic pressurized tube [26]. A. N. Eraslan and E. Arslan prisented plane strain analytical solutions to rotating partially plastic graded hollow shafts [27]. A. N. Eraslan, T. Akis presented an elastoplastic response of a long functionally graded tube subjected to internal pressure [28]. M. N. Alla, K., I.E. Ahmed, I. H. Allah presented elastic–plastic analysis of two-dimensional functionally graded materials under transient thermal loading [29]. H. Ç. Lu presented stress analysis in a functionally graded disc under mechanical loads and a steady-state temperature distribution [30]. B. H. Jahromi presented elasto-plastic stresses in a functionally graded rotating disk [31]. M. Sadeghian and H. E. Toussi presented elasto-plastic axisymmetric thermal stress analysis of the functionally graded cylindrical vessel [32].

Classical method of analysis is to combine the equilibrium equations with the stress-strain and strain- equilibrium equation's relations to arrive at the governing equation in terms of the stress components called the Navier equation. Navier equations are solved in elastic and plastic hollow FGM, analytically. The analysis is presented for two types of applicable boundary conditions. In this work, an analytical method is presented for linear plastic mechanical and thermal stress analysis for a hollow cylinder made of functionally graded materials. Temperature distribution is considered in steady-state axisymmetric case, and mechanical and thermal boundary conditions are considered in general forms. It has been assumed that the modulus of elasticity and thermal coefficient of expansion were varying through thickness of the FGM material according to a power law relationship. The Poisson's ratio was considered constant throughout the thickness.

The Navier equation is solved analytically by the direct method. Many engineering components are vulnerable to abrupt changes in the mechanical and thermal loads. Cylinders of the internal-combustion engines that are fabricated from functionally graded materials are an example of FGM cylinders, which are subjected to both internal pressure and thermal shocks. Depending on the rate of variations of applied loads and distribution of the material properties, these changes in the exerted loads may lead to the linear and perfect plastic. There are no content and sources for predicting of the linear and perfect plastic stresses in FGM cylinders until now. So, this paper is provided to predict these phenomena and let the engineers to deal with it.

2 Heat conduction problems

Consider a hollow circular cylinder of inner radius a, outer radius b made of FGM (Functionally Graded Material) respectively. The cylinder's material graded through the r-direction, thus the material properties are functions of r. Then the equation of heat conduction in steady-state condition for one-dimensional problem in polar coordinates and thermal boundary conditions for an FGM hollow cylinder yield as [3]

$$T(r) = -\frac{A_1}{m_3} r^{-m_3} + A_2 \tag{1}$$

$$\begin{aligned} c_{11}T(a) + c_{12}T_{,r}(a) &= f_1 \\ c_{21}T(a) + c_{22}T_{,r}(a) &= f_2 \end{aligned} \tag{2}$$

The coefficients of A_1 & A_2 are presented at Appendix part (A)

3 Stress analyses

3. 1 linear plastic thermal stresses

The linear plastic stress–strain relations for plane-strain conditions are

$$\begin{aligned} \epsilon_{rr} &= \frac{1}{E}\left(\sigma_{rr} - \upsilon\sigma_{\theta\theta}\right) + \alpha_0 T + \epsilon_{rr}^{p} \\ \epsilon_{\theta\theta} &= \frac{1}{E}\left(\sigma_{\theta\theta} - \upsilon\sigma_{rr}\right) + \alpha_0 T + \epsilon_{\theta\theta}^{p} \\ \epsilon_{rr}^{p} + \epsilon_{\theta\theta}^{p} &= 0 \\ \epsilon_{\theta\theta,r}^{p} + \left(\frac{\epsilon_{\theta\theta} - \epsilon_{rr}}{r}\right) &= 0 \end{aligned} \tag{3}$$

Where (,r) denotes differentiation with respect to r. where σ_{ij} and ϵ_{ij} (i, j = r, ϴ) are the stress and strain tensors, T is the temperature distribution determined from the heat conduction equation, α is the coefficient of thermal expansion, and λ and μ are Lame´ coefficients related to the modulus of elasticity E and Poisson's ratio υ as

$$\begin{aligned} \lambda &= \frac{\upsilon E}{(1+\upsilon)(1-2\upsilon)} \\ \mu &= \frac{E}{2(1+\upsilon)} \end{aligned} \tag{4}$$

The equilibrium equation in the radial direction, disregarding the body force and the inertia term, is

$$\sigma_{rr,r}+\left(\frac{\sigma_{rr}-\sigma_{\theta\theta}}{r}\right)=0 \tag{5}$$
$$\sigma_{\theta\theta}=r\sigma_{rr,r}+\sigma_{rr}$$

To obtain the equation of stresses in terms of plastic strain for the FGM cylinder the functional relationship of the material properties must be known. Since the cylinder's material is assumed to be graded along the r direction, the modulus of elasticity and the coefficient of thermal expansion and yield strength are assumed to be described as a power law as.

$$\alpha=\alpha_0\left(\frac{R}{l}\right)^{m_1}=\alpha_0 r^{m_1}$$
$$\alpha=\alpha_0\left(\frac{R}{l}\right)^{m_1}=\alpha_0 r^{m_1}$$
$$\sigma_0=\sigma_0(\frac{R}{l})^{m_4}=\sigma_0 r^{m_4} \tag{6}$$

Where E_0 and α_0 and σ_{0r} are the material constants and m_1, m_2, m_3 and m_4 are the power law indices of the material. We may further assume that Poisson's ratio is constant.
Using relations (3)–(6), the Navier equation in terms of the stresses is.

$$\sigma_{rr,rr}+(3-m_1)\frac{1}{r}\sigma_{rr,r}+m_1(\upsilon-1)\frac{1}{r^2}\sigma_{rr}=-m_2\alpha_0E_0r^{m_1+m_2-2}T-\alpha_0E_0r^{m_1+m_2-1}T_{,r}+E_0r^{m_1-1}\epsilon^p_{rr,r}+2E_0r^{m_1-2}\epsilon^p_{rr} \tag{7}$$

Substituting Eq. (1) into Eq. (7) yields

$$\sigma_{rr,rr}+g_1\frac{1}{r}\sigma_{rr,r}+g_2\frac{1}{r^2}\sigma_{rr}=g_3r^{m_1+m_2-2}T+g_4r^{m_1+m_2-1}T_{,r}+g_5r^{m_1-1}\epsilon^p_{rr,r}+g_6r^{m_1-2}\epsilon^p_{rr} \tag{8}$$

The coefficients of Eq (8) are presented at Appendix part (A). Eq (8) is the differential equation with general and particular solutions. The general solution is assumed to have the form.

$$\sigma^g_{rr}(r)=Ir^z \tag{9}$$

Substituting Eq. (9) into Eq. (8) yields

$$z^2+z(g_1-1)+g_2=0 \tag{10}$$

Eq. (10) has two real roots z_1 and z_2 :

$$z_1=\frac{-(g_1-1)}{2}+(\frac{(g_2-1)^2}{2}-g_2)^{0.5}$$
$$z_2=\frac{-(g_1-1)}{2}-(\frac{(g_2-1)^2}{2}-g_2)^{0.5} \tag{11}$$

Thus the general solution is as written below:

$$\sigma_{rr}^{g}\left(r\right)=I_1 r^{z_1}+I_2 r^{z_2} \tag{12}$$

The particular solution $\sigma_{rr}^{g}\left(r\right)$ is assumed to be of the form as below:

$$\sigma_{rr}^{p}\left(r\right)=H_1 r^{m_1+m_2-m_3}+H_2 r^{m_1+m_2}+H_3\epsilon_{rr,r}^{p} r^{m_1+1}+H_4\epsilon_{rr}^{p} r^{m_1} \tag{13}$$

By substituting Eq. (13) into Eq. (8) equating the coefficients of the identical power yields and they are presented at Appendix part (A). The complete solution for σ_{rr} is the sum of the general and particular solutions as

$$\sigma_{rr}=I_1 r^{z_1}+I_2 r^{z_2}+H_1 r^{m_1+m_2-m_3}+H_2 r^{m_1+m_2}+H_3\epsilon_{rr,r}^{p} r^{m_1+1}+H_4\epsilon_{rr}^{p} r^{m_1} \tag{14}$$

And the hoop stress become as

$$\sigma_{\theta\theta}=(z_1 I_1+I_1)\mathrm{r}^{z_1}+(z_2 I_2+I_2)\mathrm{r}^{z_2}+\left[\left(m_1+m_2-m_3\right)H_1+H_1\right]r^{m_1+m_2-m_3}+\left[\left(m_1+m_2\right)H_2+H_2\right]r^{m_1+m_2}+$$
$$\left[\left(m_1+1\right)H_3\epsilon_{rr,r}^{p}+H_3\epsilon_{rr,r}^{p}+H_4\epsilon_{rr,r}^{p}\right]r^{m_1+1}+\left[H_3\epsilon_{rr,rr}^{p}\right]r^{m_1+2}+\left[m_1 H_4\epsilon_{rr}^{p}+H_4\epsilon_{rr}^{p}\right]r^{m_1} \tag{15}$$

To determine the constants I_1 and I_2; consider the boundary conditions for stresses given by

$$\sigma_{rr}(a)=0$$
$$\sigma_{rr}(b)=0 \tag{16}$$

Substituting the boundary conditions (16) into Eq. (14), the constants of integration for thermal stress yield, and they are presented at Appendix part (A).
The elastic stresses are [3]

$$\sigma_{rr}=\frac{\mathrm{E}_0}{(1+\upsilon)(1-2\upsilon)}[\left(\left(1-\nu\right)\eta_1+\nu\right)B_1 r^{m_1+\eta_1-1}+\left(\left(1-\nu\right)\eta_2+\nu\right)B_2 r^{m_1+\eta_1-1}+(\left(\left(1-\nu\right)m_2+1\right)D_1-$$
$$\left(1+\nu\right)\alpha_0 A_2)r^{m_1+m_2}+(((1-\nu)(\mathrm{m}_2-\mathrm{m}_3)+1)\mathrm{D}_2+\frac{(1+\nu)\alpha_0 A_1}{m_3})r^{m_1+m_2+m_3}]$$

$$\sigma_{\theta\theta}=\frac{\mathrm{E}_0}{(1+\upsilon)(1-2\upsilon)}[\left(\left(1-\nu\right)+\eta_1\nu\right)B_1 r^{m_1+\eta_1-1}+\left(\left(1-\nu\right)+\eta_2\nu\right)B_2 r^{m_1+\eta_1-1}+(\left(\nu m_2+1\right)D_1-$$
$$\left(1+\nu\right)\alpha_0 A_2)r^{m_1+m_2}+((\nu(\mathrm{m}_2-\mathrm{m}_3)+1)\mathrm{D}_2+\frac{(1+\nu)\alpha_0 A_1}{m_3})r^{m_1+m_2+m_3}] \tag{17}$$

In terms of a graph of (ϵ_{rr}^{p}, s) the gradient (M*E) of a graph is obtained. Then the equation of linear plastic strain for thermal stresses yields as [33]

$$\epsilon_{rr}^{p}=\frac{1-M}{M}\left(1-s\right)$$

$$s=s_{rr}-s_{\theta\theta}$$

$$s_{rr} = \frac{\sigma_{rr}}{\sigma_0 r^{m_4}}$$

$$s_{\theta\theta} = \frac{\sigma_{\theta\theta}}{\sigma_0 r^{m_4}} \tag{18}$$

By substituting Eq. (17) into Eq. (18) the ϵ_{rr}^{p} yields as

$$\epsilon_{rr}^{p} = \frac{1-M}{M}(-1+\frac{\mathrm{E}_0}{(1+\upsilon)(1-2\upsilon)\sigma_0}[(1-\eta_1)(1-2v)B_1 r^{m_1+\eta_1-1-m_4}+(1-\eta_2)(1-2v)B_2 r^{m_1+\eta_1-1-m_4}+$$
$$(D_1 m_2(2v-1)r^{m_1+m_2-m_4}+((m_2-m_3)(2vD_2-D_2))r^{m_1+m_2-m_3-m_4})]) \tag{19}$$

From equation (18) the $\epsilon_{rr,r}^{p}$ yields as

$$\epsilon_{rr,r}^{p} = \frac{M-1}{M}(S_{,r}) \tag{20}$$

From equation (5) S yields as

$$S = -rS_{rr,r}$$
$$S_{,r} = -S_{rr,r} - S_{rr,rr} \tag{21}$$

By substituting equation (21) into the equation (20) the $\epsilon_{rr,r}^{p}$ yields as

$$\epsilon_{rr,r}^{p} = \frac{M-1}{M}(-s_{r,r} - S_{rr,rr})$$
$$S_{,r} = -\frac{1}{\sigma_0 r^{m_4}}(\sigma_{rr})_{,r} - r(\frac{\sigma_{rr,r}}{\sigma_0 r^{m_4}})_{,r} \tag{22}$$

3.2 Linear plastic mechanical stresses

Substituting Eq. (3) into Eq. (6) without considering the thermal boundary conditions the equation of elastic stress yields

$$\sigma_{rr,rr} + g_1\frac{1}{r}\sigma_{rr,r} + g_2\frac{1}{r^2}\sigma_{rr} = g_5 r^{m_1-1}\epsilon_{rr,r}^{p} + g_6 r^{m_1-2}\epsilon_{rr}^{p} \tag{23}$$

After solving Eq. (23) such as solving equation of thermal stresses, mechanical stresses yield as

$$\sigma_{rr} = K_1 r^{z_1} + K_2 r^{z_2} + H_3\epsilon_{rr,r}^{p} r^{m_1+1} + H_4\epsilon_{rr}^{p} r^{m_1}$$

$$\sigma_{\theta\theta} = (z_1 K_{1+} K_1)r^{z_1} + (z_2 K_{2+} K_2)r^{z_2} + [(\mathrm{m}_1+1)H_3\epsilon_{rr,r}^{p} + H_3\epsilon_{rr,r}^{p} + H_4\epsilon_{rr,r}^{p}]r^{m_1+1} + H_3\epsilon_{rr,rr}^{p} r^{m_1+2} +$$
$$[m_1 H_4\epsilon_{rr}^{p} + H_4\epsilon_{rr}^{p}]r^{m_1} \tag{24}$$

To determine the constants K_1 and K_2; consider the boundary conditions for stresses given by

$$\sigma_{rr}(a) = -p_i$$
$$\sigma_{rr}(b) = 0 \tag{25}$$

Substituting the boundary conditions (25) into Eq. (24), the constants of integration for mechanical stress yield, and they are presented at Appendix part (B).
The elastic mechanical stresses are [3]

$$\sigma_{rr} = \frac{E_0}{(1+\upsilon)(1-2\upsilon)}[\left((1-\nu)\eta_1+\nu\right)B_1 r^{m_1+\eta_1-1} + \left((1-\nu)\eta_2+\nu\right)B_2 r^{m_1+\eta_1-1}$$
$$\sigma_{\theta\theta} = \frac{E_0}{(1+\upsilon)(1-2\upsilon)}[\left((1-\nu)+\eta_1\nu\right)B_1 r^{m_1+\eta_1-1} + \left((1-\nu)+\eta_2\nu\right)B_2 r^{m_1+\eta_1-1} \tag{26}$$

In terms of a graph of (ϵ_{rr}^{p}, s) the gradient (M*E) of a graph is obtained. Then the equation of linear plastic strain for mechanical stresses yields as [33]

$$\varepsilon_{rr}^{p} = \frac{1-M}{M}(-1-s) \tag{27}$$

From equation (27) the $\epsilon_{rr,r}^{p}$ yields as

$$\varepsilon_{rr,r}^{p} = \frac{M-1}{M}(s_{,r}) \tag{28}$$

3-3 Critical temperature

The critical temperature is a temperature that causes the stresses to go beyond the elastic region and come to plastic criteria. So this is one of the more important factors in designing. The constants of integration for elastic stresses are presented at Appendix part (c) [3].
For obtaining the critical temperature the Tresca's criterion is shown as [33]

$$\left|\sigma_{\theta\theta} - \sigma_{rr}\right| = \sigma_0 r^{m_4} \tag{29}$$

By substituting the equation (17) into equation (29), equation (30) yields as

$$\left|\begin{array}{l}\frac{E_0}{(1+\upsilon)(1-2\upsilon)}[(1-\eta_1)(1-2\nu)B_1 r^{m_1+\eta_1-1} + (1-\eta_2)(1-2\nu)B_2 r^{m_1+\eta_2-1} + \\ (D_1 m_2(2\nu-1)r^{m_1+m_2} + (m_2-m_3)(2\nu D_2 - D_2))r^{m_1+m_2-m_3}]\end{array}\right| = \sigma_0 r^{m_4} \tag{30}$$

By substituting the equations that are presented at Appendix part (C) & (D) into Eq. (30), the Tresca's criterion become as

$$\left|(d_{22}d_{26}r^{m_1+\eta_1-1} + d_{23}d_{20}r^{m_1+\eta_2-1} + d_{24}A_8 r^{m_1+m_2} + -d_{25}A_{10}r^{m_1+m_2-m_3})\,f_2 + (d_{22}d_{27} + d_{23}d_{21} + d_{22}A_{10}r^{m_1+m_2-m_3})\,f_1\right| = \sigma_0 r^{m_4} \tag{31}$$

The coefficients of f_1 and f_2 are as inner & outer critical temperatures.

3-4 Critical Pressures

The critical pressure is a pressure that causes the stresses to go beyond the elastic region and come to plastic criteria. By substituting equation (26) into the equation (29) the critical pressure yields as

$$P_0\left(\frac{r^{m_1+\eta_1-1}a^{m_1+\eta_2-1}\left(1-\frac{v\eta_1+1-v}{(1-v)\eta_1+v}\right)+r^{m_1+\eta_2-1}a^{m_1+\eta_1-1}\frac{v\eta_2+1-v}{(1-v)\eta_2+v}-1}{a^{m_1+\eta_1-1}b^{m_1+\eta_2-1}-a^{m_1+\eta_2-1}b^{m_1+\eta_1-1}}\right)-$$
$$P_i\left(\frac{r^{m_1+\eta_1-1}b^{m_1+\eta_2-1}\left(-1+\frac{v\eta_1+1-v}{(1-v)\eta_1+v}\right)+r^{m_1+\eta_2-1}a^{m_1+\eta_1-1}\frac{v\eta_2+1-v}{(1-v)\eta_2+v}-1}{a^{m_1+\eta_1-1}b^{m_1+\eta_2-1}-a^{m_1+\eta_2-1}b^{m_1+\eta_1-1}}\right)+$$
$$\frac{r^{\eta_2+m_1-1}b^{\eta_1+m_1-1}\left(1-\frac{\upsilon\eta_2+1-\upsilon}{(1-\upsilon)\eta_2+\upsilon}\right)}{a^{\eta_1+m_1-1}b^{\eta_2+m_1-1}-a^{\eta_2+m_1-1}b^{\eta_1+m_1-1}}\Bigg)=\sigma_0 r^{m_4}$$

(32)

We obtain, P_i and P_0 as inner & outer critical pressure.

The limitations of analytical method for this paper are assumed as below:

The Poisson's ratio is considered constant. To determine the constants I_1 and I_2; the boundary conditions for stresses is assumed $\sigma_{rr}(a)=0$ and $\sigma_{rr}(b)=0$. The modulus of elasticity and the coefficient of thermal expansion and yield strength are assumed to be described as a power law.

4 Result and discussion

As an example1, consider a thick hollow cylinder of inner radius a = 1 m, and outer radius b = 1.2 m, Poisson's ratio is taken to be 0.3, and the modulus of elasticity and the thermal coefficients of expansion at the inner radius are $E_i=200$ Gpa, and $\alpha_i=1.2*10^{-6}/^{\circ}\mathrm{c}$, respectively. For simplicity of analysis, the power law coefficients for k, E and α coefficient are considered to be the same, i.e. $m_1=m_2=m_3=m_4=m$. The boundary conditions for temperature are taken as $T(a)=T_i{}^{\circ}\mathrm{c}$ and $T(b)=T_o{}^{\circ}\mathrm{c}$.

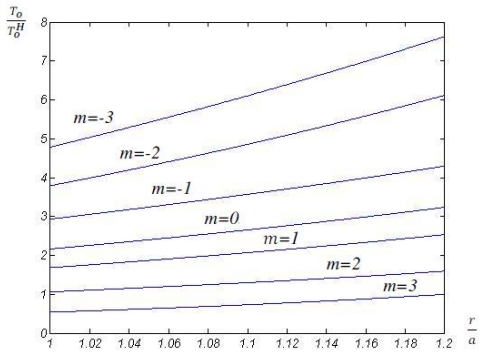

Figure (1-a) Outer critical temperature distribution of radial when T_i=P_i=P_o=0

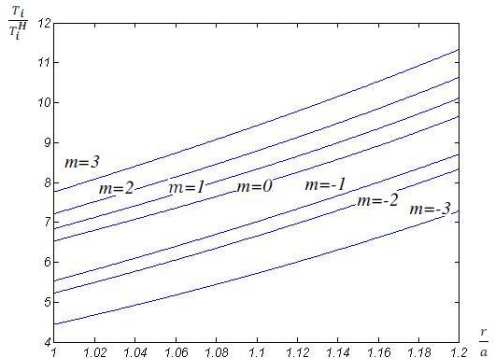

Figure (1-b) Inner critical temperature distribution of radial when T_o=P_i=P_o=0

The hollow cylinder has pressure on its inner surface so the boundary conditions for thermal stresses are assumed as $\sigma_{rr}(a)=0$ and $\sigma_{rr}(b)=0$ and for the second example, mechanical stresses are assumed as $\sigma_{rr}(a)=-50$ Mpa, and $\sigma_{rr}(b)=0$ for earning the critical pressure we considered $P(a)=-P_i$ Mpa, and $P(b)=P_o$ Mpa. As an example 3, consider a thick hollow cylinder of inner radius $a=0.7$ m and outer radius $b=1$ m, $\frac{p_i}{p_o}=0.33$, the power law coefficient for $m=0.6$ and the other coefficients are same as the previous example. Figure (1-a) shows the outer critical temperature distribution of radial, when $T_i=P_i=P_o=0$. The effect of the power-law index to the distribution of the outer critical temperature radial is shown in this figure. Figure (1-b) shows the inner critical temperature distribution of radial, when $T_o=P_i=P_o=0$. These figures show increasing the power-law index cause to increase the inner critical temperature and decrease the outer critical temperature. Figure (2-a) shows the outer critical pressure distribution of radial, when $T_o=T_i=P_i=0$. Also you can see the effect of power-law index to the distribution of the outer critical pressure is shown in this figure. Figure (2-b) shows the inner critical pressure distribution of radial when $T_o=T_i=P_o=0$ and effect of power-law index to the distribution of the outer critical pressure. Figure (3-a) shows the outer pressure for all over the cylinder goes to plastic region, when $T_o=T_i=P_o=0$. Figure (3-b) shows the radial inner pressure for all over the cylinder goes to the plastic region when $T_o=T_i=P_o=0$. Figure (4-a) shows the radial thermal stress of linear plastic for m=1 when $T_o=P_i=P_o=0$ & T_i=200$^{\circ}_{c}$ and the effect of any gradients on it.

Figure (4-b) shows the linear plastic' radial thermal stress for m=-1 when $T_o=P_i=P_o=0$ & $T_i=200°c$ and the effect of the gradient on linear plastic' radial thermal stress. Figure (5-a) shows the Circumferential thermal stress of linear plastic for m=1 when $T_o=P_i=P_o=0$ & $T_i=200°c$ and the effect of the gradient on linear plastic' circumferential thermal stress. Figure (5-b) shows the Circumferential thermal stress of linear plastic for m=-1 when $T_o=P_i=P_o=0$, $T_i=200°c$ and the effect of the gradient on linear plastic' circumferential thermal stress. Figure (6-a) shows the effective thermal stress of linear plastic for m=1 when $T_o=P_i=P_o=0$ & $T_i=200°c$ and the effect of M index on it.

Figure (6-b) shows the effective thermal stress of linear plastic for m=-1 when $T_o=P_i=P_o=0$ & $T_i=200°c$ and the effect of M index on it. Figure (7-a) indicates the comparing of radial elastic stress [3] (shows with square) with linear plastic stress by substituting $\epsilon^{p}_{rr}=\epsilon^{p}_{rr,r}=0$ in stress formula that they should be the same because by putting $\epsilon^{p}_{rr}=\epsilon^{p}_{rr,r}=0$ in radial linear plastic stress it turns to radial elastic stress.

Figure (7-b) shows the radial mechanical stress of linear plastic for m=1 when $T_o=T_i=P_i=0$ & $P_i=-50$ Mpa and the effect of M on radial mechanical stress of linear plastic. Figure (8-a) indicates the radial mechanical stress of linear plastic for m=-1 when $T_o=T_i=P_o=0$ & $P_i=-50$ Mpa and the effect of M on radial mechanical stress of linear plastic. Figure (8-b) shows the comparing of radial plastic stress [28] (shows with square) with radial linear plastic by substituting M=0. By substituting M=0 in radial linear plastic stress formula it turns to perfect plastic when $T_o=T$ & $\frac{p_i}{p_o}=0.33$ Mpa.

The thing that justifies the difference of two graphs is that in that article, they considered yield strength as constant but in this article, yield strength is depended on radius and power law's coefficient. Figure (9-a) shows the circumferential mechanical stress of linear plastic for m=-1 when $T_o = P_i = P_o = 0$ & $P_i = -50$ Mpa and the effect of M on circumferential mechanical stress of linear plastic. Figure (9-b) shows the effective mechanical stress of linear plastic for m=-1 when $T_o = T_i = P_i = 0$ & $P_i = -50$ Mpa and the effect of M on circumferential mechanical stress of linear plastic. Figure (10-a) shows the radial mechanical stress for the whole of the cylinder goes to the plastic region causes by P_i for m=1 when $T_o = P_i = P_o = 0$. Figure (10-b) indicates the circumferential mechanical stress for the whole of the cylinder goes to the plastic region causes by P_i for m=1 when $T_o = P_i = P_o = 0$. Figure (11-a) indicates the effective mechanical stress for the whole of the cylinder goes to the plastic region causes by P_i for m=1 when $T_o = P_i = P_o = 0$.

Figure (11-b) shows the radial mechanical stress for the whole of the cylinder goes to the plastic region causes by P_i for m=-1 when $T_o = P_i = P_o = 0$. Figure (12-a) shows the circumferential mechanical stress for the whole of the cylinder goes to the plastic region causes by P_i for m=-1 when $T_o = P_i = P_o = 0$. Figure (12-b) indicates the effective mechanical stress for the whole of the cylinder goes to the plastic region causes by P_i for m=-1 when $T_o = P_i = P_o = 0$. Figure (13-a) shows the radial mechanical stress for half of a cylinder goes to plastic region causes by p_i for m=1 when $T_o = P_i = P_o = 0$. Figure (13-b) shows the radial mechanical stress for half of a cylinder goes to plastic region causes by P_i for m=-1 when $T_o = P_i = P_o = 0$. Figure (14-a) shows the circumferential mechanical stress for half of a cylinder goes to plastic region causes by P_i for m=-1 when $T_o = P_i = P_o = 0$. What can infer about this graph is that in terms of each M, the stress has a new yield point. Figure (14-b) indicates the effective mechanical stress for a half of cylinder goes to plastic region causes by P_i for m=-1 when $T_o = P_i = P_o = 0$. Figure (15-a) indicates the radial mechanical stress for the whole of a cylinder goes to the plastic region causes by P_o for m=1 when $T_o = T_i = P_i = 0$. Figure (15-b) indicates the circumferential mechanical stress for the whole of a cylinder goes to the plastic region causes by p_o for m=1 when $T_o = T_i = P_i = 0$. Figure (16-a) indicates the effective mechanical stress for the whole of a cylinder goes to the plastic region causes by P_o for m=1 when $T_o = T_i = P_i = 0$. Figure (16-b) indicates the radial mechanical stress for the whole of a cylinder goes to the plastic region causes by P_o for m=-1 when $T_o = T_i = P_i = 0$. Figure (17-a) indicates the circumferential mechanical stress for the whole of a cylinder goes to plastic region causes by P_o for m=-1 when $T_o = T_i = P_i = 0$. Figure (17-b) indicates the effective mechanical stress for the whole of a cylinder goes to the plastic region causes by p_o for m=-1 when $T_o = T_i = P_i = 0$. Figure (18-a) indicates the radial mechanical stress for the half of a cylinder goes to the plastic region causes by p_o for m=1 when $T_o = T_i = P_i = 0$. Figure (18-b) indicates the radial mechanical stress for half of cylinder goes to plastic region causes by P_o for m=-1 when $T_o = T_i = P_i = 0$. Figure (19-a) indicates the circumferential mechanical stress for half of cylinder goes to plastic region causes by p_o for m=-1 when $T_o = T_i = P_i = 0$. Figure (19-b) indicates the effective mechanical stress for the half of a cylinder goes to the plastic region causes by P_o for m=-1 wen $T_o = T_i = P_i = 0$.

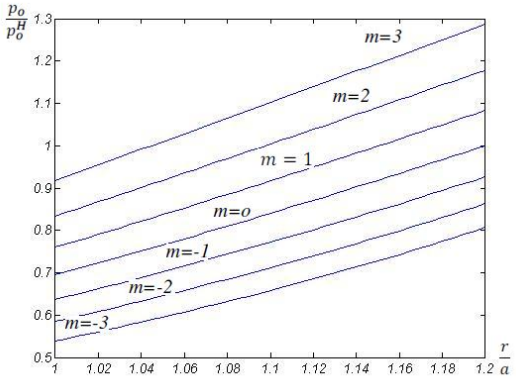

Figure (2-a) Outer critical pressure distribution of radial when T_i=T_o=P_o=0

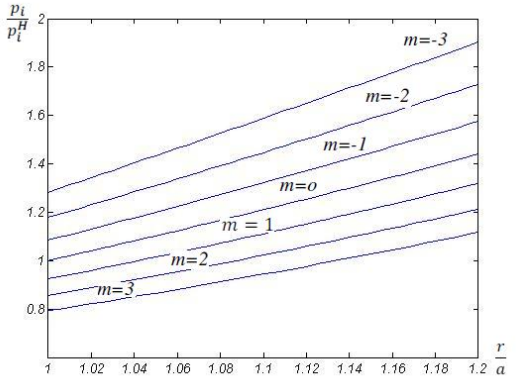

Figure (2-b) Inner critical pressure distribution of radial when T_i=T_o=P_o=0

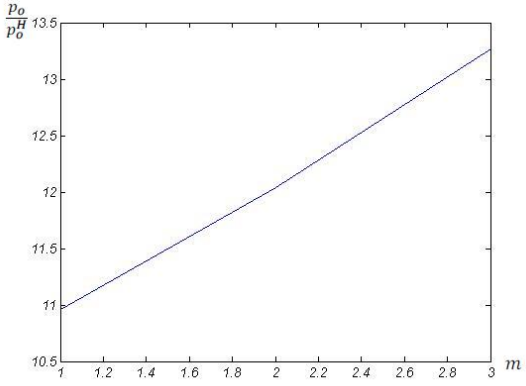

Figure (3-a) Outer pressure for all over the cylinder goes to plastic region when T_i=T_o=P_i=0

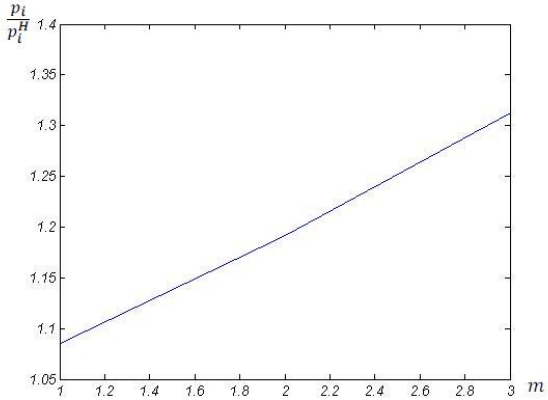

Figure (3-b) Inner pressure for all over the cylinder goes to plastic region when T_i=T_o=P_o=0

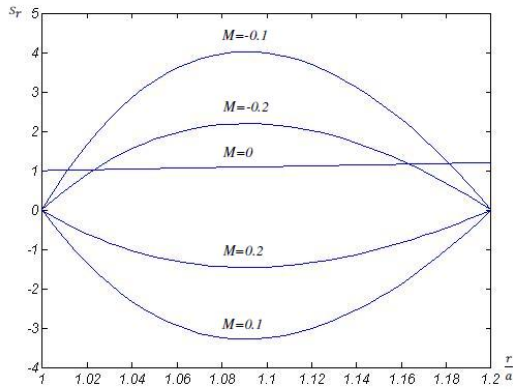

Figure (4-a) Radial thermal stress of linear plastic for m=1 when T_o=P_i=P_o=0 & T_i=200$^{\circ}_c$

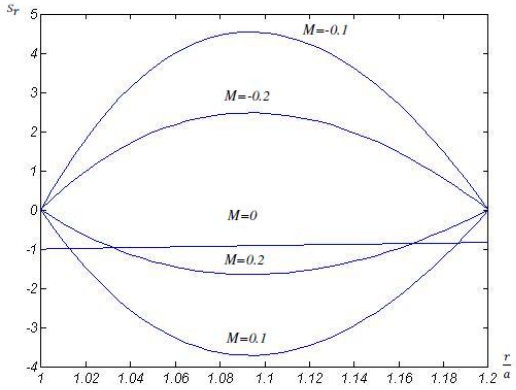

Figure (4-b) Radial thermal stress of linear plastic for m=-1 when T_o=P_i=P_o=0 & T_i=200$^{\circ}_c$

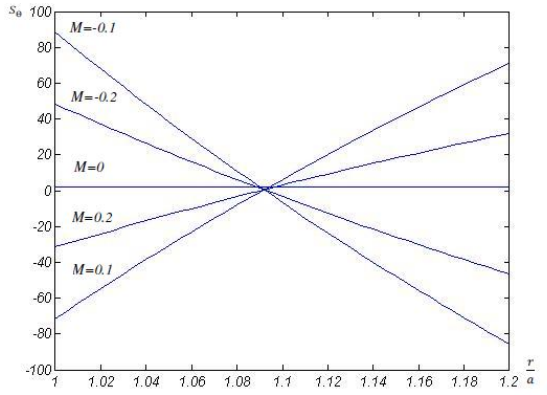

Figure (5-a) Circumferential thermal stress of linear plastic for m=1 when when T_o=P_i=P_o=0 & T_i=200$^\circ_c$

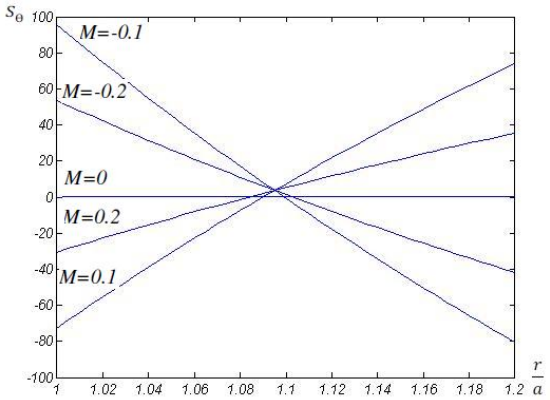

Figure (5-b) Circumferential thermal stress of linear plastic for m=-1 when when T_o=P_i=P_o=0 & T_i=200$^\circ_c$

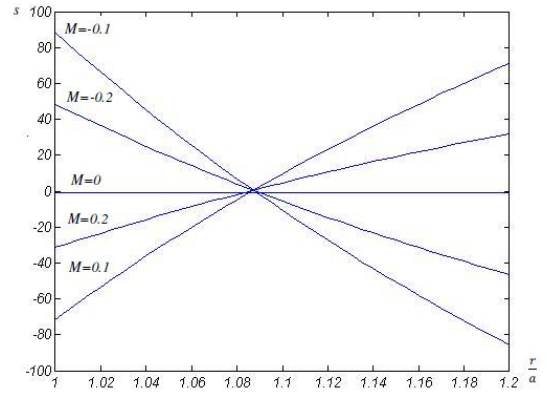

Figure (6-a) Effective thermal stress of linear plastic for m=1 when T_o=P_i=P_o=0 & T_i=200$^\circ_c$

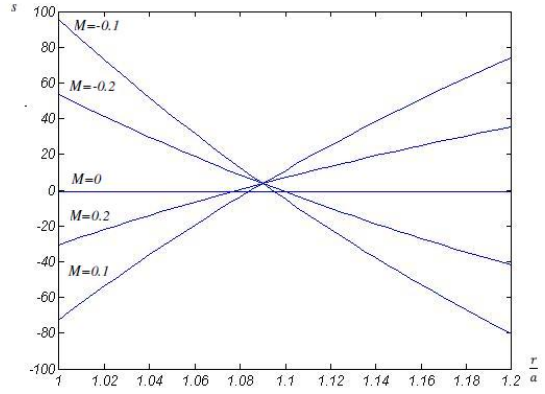

Figure (6-b) Effective thermal stress of linear plastic for m=-1 when T_o=P_i=P_o=0 & T_i=200$^\circ_c$

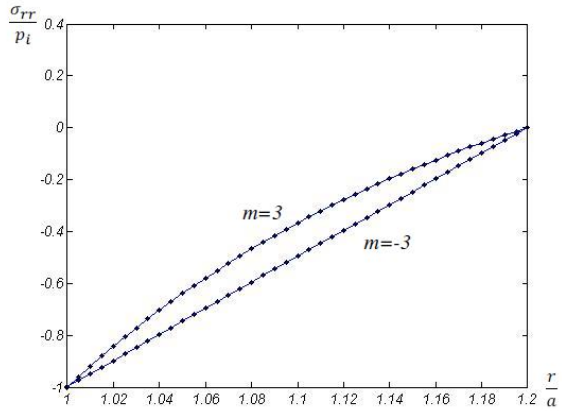

Figure (7-a) Comparing of radial elastic stress [3] (shows with square) with linear plastic stress by substituting ϵ^p_{rr}= $\epsilon^p_{rr,r}$=0 in stress formula that they should be the same when T_o=P_o=0 & T_i=10$^\circ_c$ & P_i =-50 Mpa

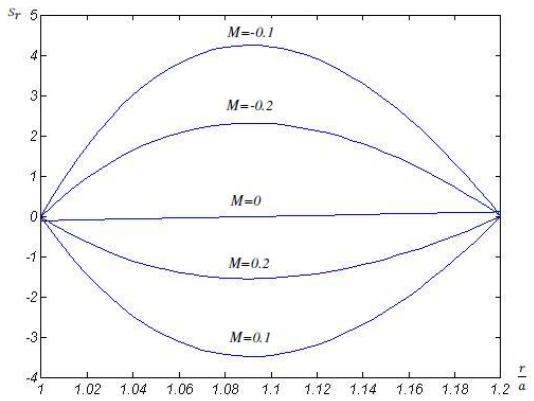

Figure (7-b) Radial mechanical stress of linear plastic for m=1 when T_o=T_i=P_o=0 & P_i=-50 Mpa

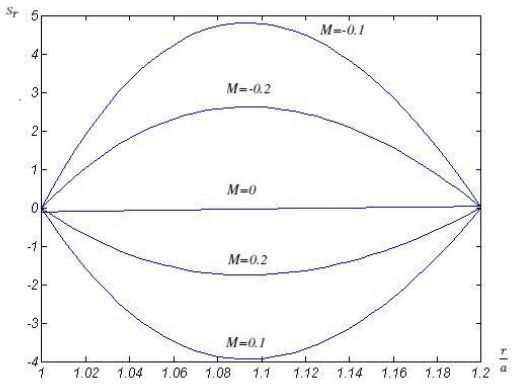

Figure (8-a) Radial mechanical stress of linear plastic for m=-1 when T_o=T_i=P_o=0 & P_i=-50 Mpa

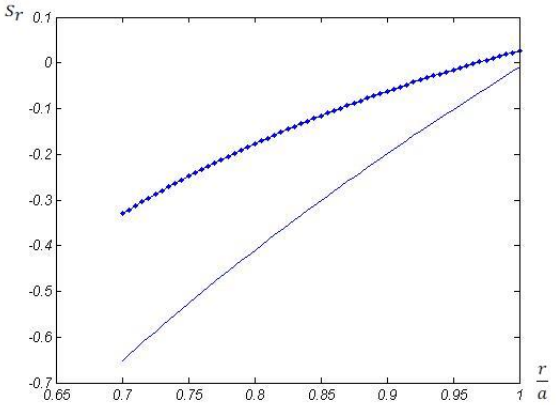

Figure (8-b) Comparing of radial plastic stress [28](shows with square) with radial linear plastic by substituting M=0 when T_o=T_i & $\frac{p_i}{p_o}$=.33 Mpa

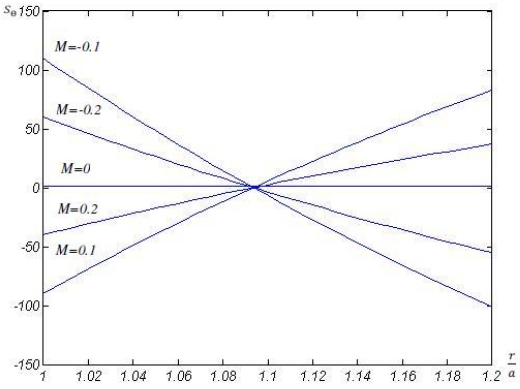

Figure (9-a) Circumferential mechanical stress of linear plastic for m=-1 when T_o=T_i=P_o=0 & P_i=-50 Mpa

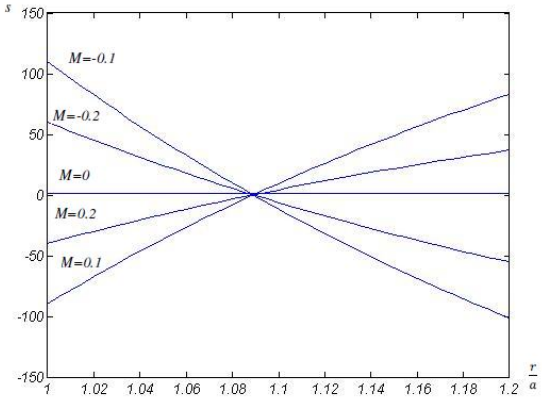

Figure (9-b) Effective mechanical stress of linear plastic for m=-1 when T_o=T_i=P_o=0 & P_i=-50 Mpa

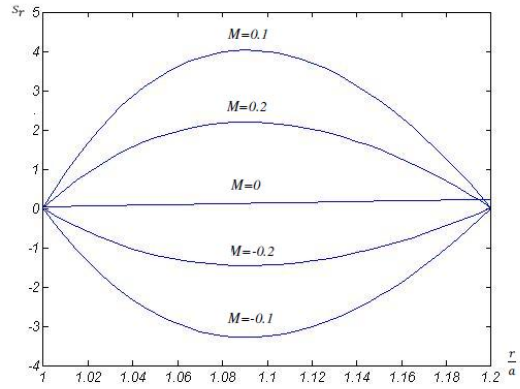

Figure (10-a) Radial mechanical stress for whole of cylinder goes to plastic region causes by p_i for m=1 when T_o=T_i=P_o=0

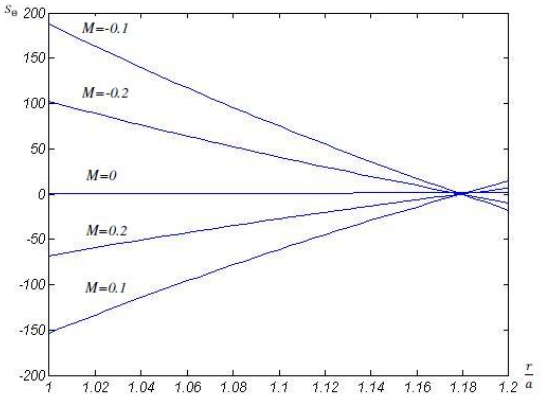

Figure (10-b) Circumferential mechanical stress for whole of cylinder goes to plastic region causes by p_i for m=1when T_o=T_i=P_o=0

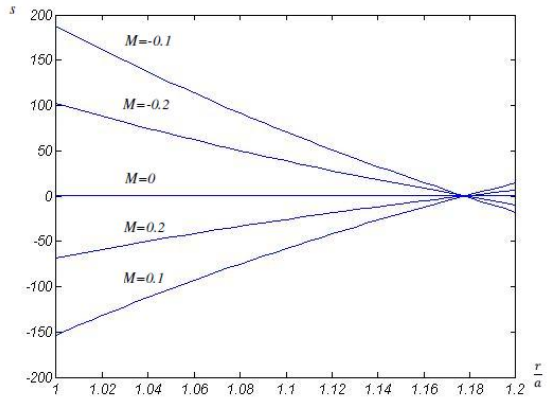

Figure (11-a) Effective mechanical stress for whole of cylinder goes to plastic region causes by p_i for m=1 when T_o=T_i=P_o=0

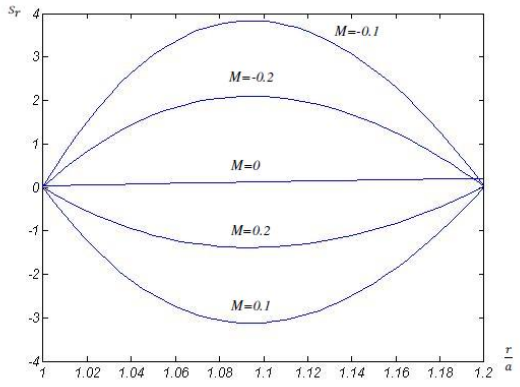

Figure (11-b) Radial mechanical stress for whole of cylinder goes to plastic region causes by p_i for m=-1 when T_o=T_i=P_o=0

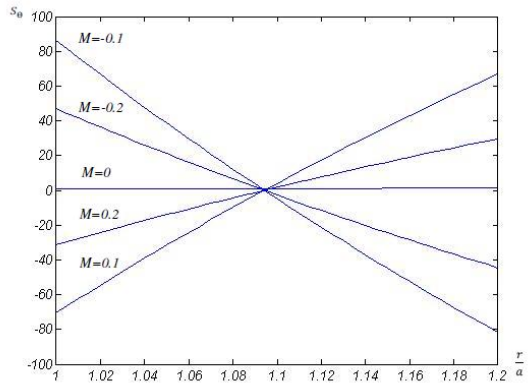

Figure (12-a) Circumferential mechanical stress for whole of cylinder goes to plastic region causes by p_i for m=-1 when T_o=T_i=P_o=0

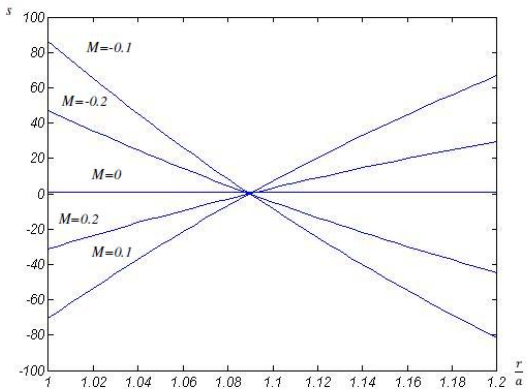

Figure (12-b) Effective mechanical stress for whole of cylinder goes to plastic region causes by p_i for m=-1 when T_o=T_i=P_o=0

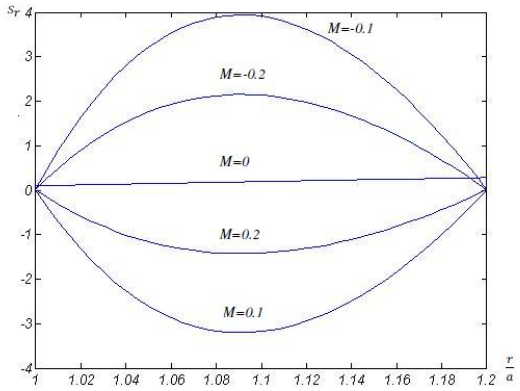

Figure (13-a) Radial mechanical stress for half of cylinder goes to plastic region causes by p_i for m=1 when T_o=T_i=P_o=0

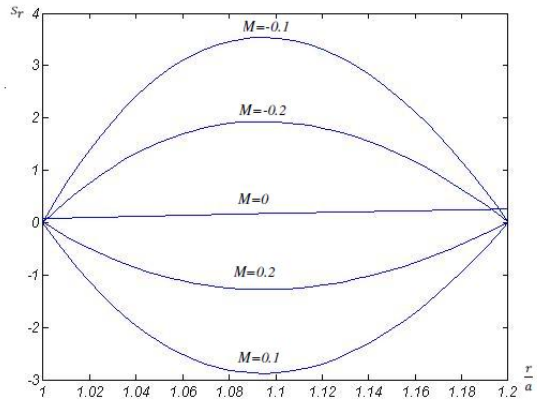

Figure (13-b) Radial mechanical stress for half of cylinder goes to plastic region causes by p_i for m=-1 when T_o=T_i=P_o=0

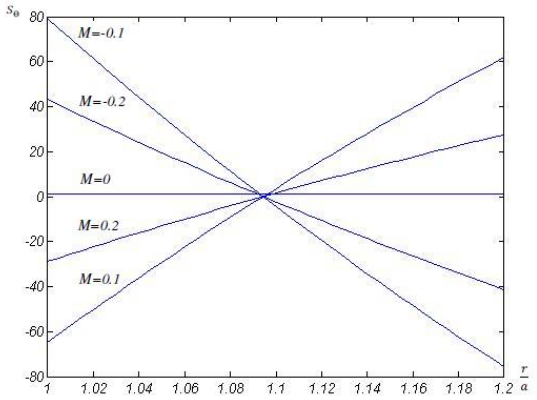

Figure (14-a) Circumferential mechanical stress for half of cylinder goes to plastic region causes by p_i for m=-1 when T_o=T_i=P_o=0

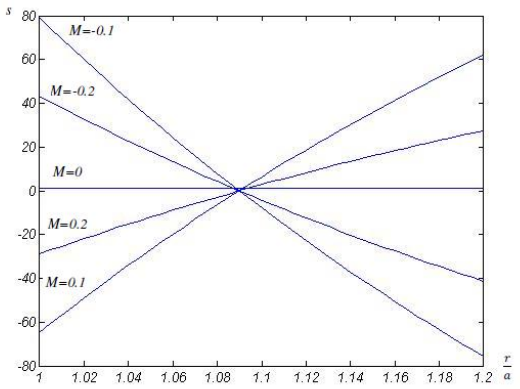

Figure (14-b) Effective mechanical stress for half of cylinder goes to plastic region causes by p_i for m=-1 when T_o=T_i=P_o=0

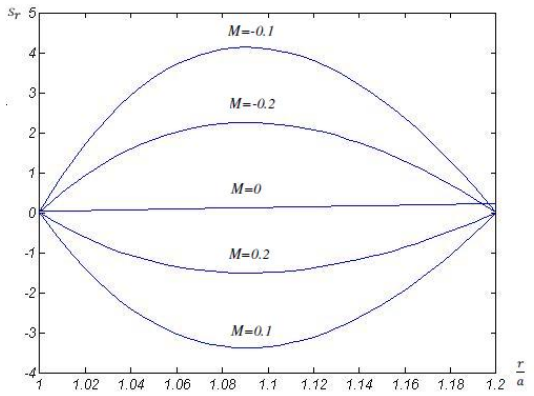

Figure (15-a) Radial mechanical stress for whole of cylinder goes to plastic region causes by p_o for m=1 when T_o=T_i=P_i=0

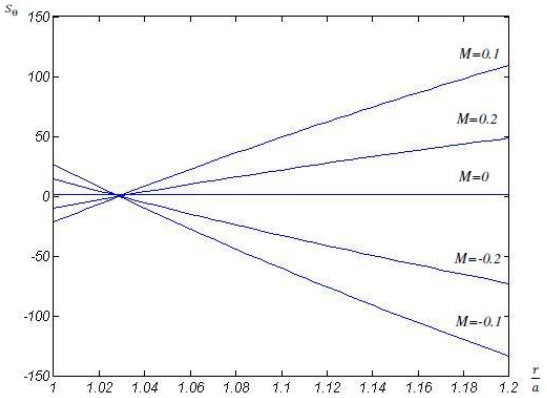

Figure (15-b) Circumferential mechanical stress for whole of cylinder goes to plastic region causes by p_o for m=1 when T_o=T_i=P_i=0

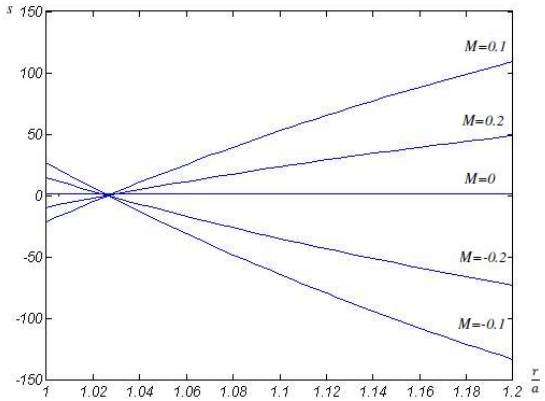

Figure (16-a) Effective mechanical stress for whole of cylinder goes to plastic region causes by p_o for m=1 when T_o=T_i=P_i=0

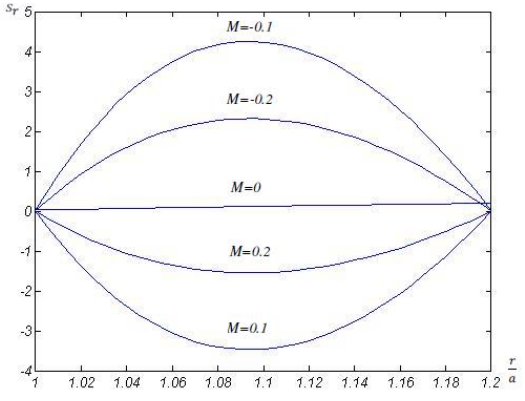

Figure (16-b) Radial mechanical stress for whole of cylinder goes to plastic region causes by p_o for m=-1 when T_o=T_i=P_i=0

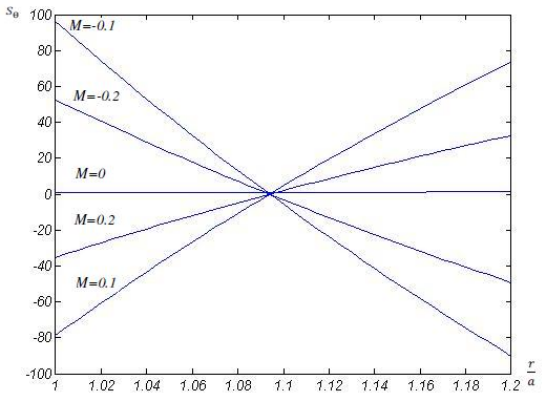

Figure (17-a) Circumferential mechanical stress for whole of cylinder goes to plastic region causes by p_o for m=-1 when T_o=T_i=P_i=0

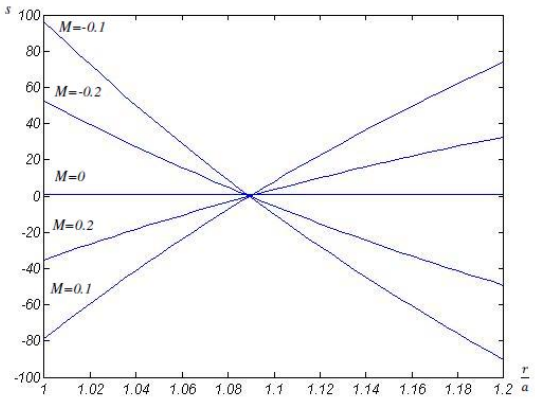

Figure (17-b) Effective mechanical stress for whole of cylinder goes to plastic region causes by p_o for m=-1 when T_o=T_i=P_i=0

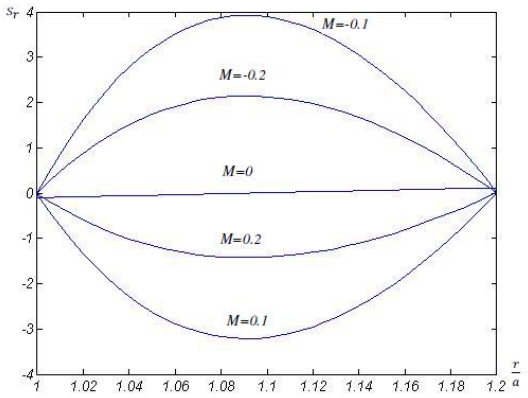

Figure (18-a) Radial mechanical stress for half of cylinder goes to plastic region causes by p_o for m=1 when T_o=T_i=P_i=0

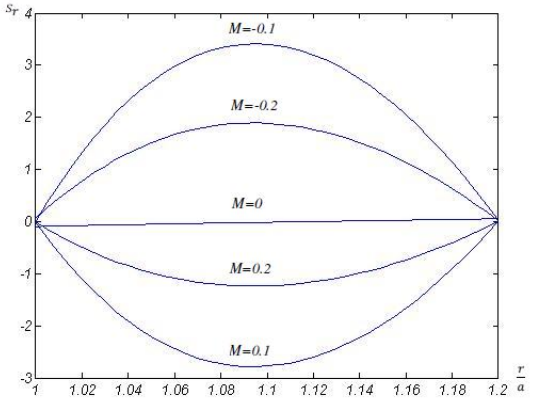

Figure (18-b) Radial mechanical stress for half of cylinder goes to plastic region causes by p_o for m=-1 when T_o=T_i=P_i=0

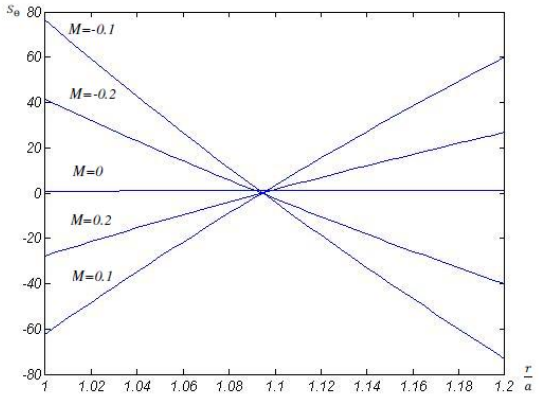

Figure (19-a) Circumferential mechanical stress for half of cylinder goes to plastic region causes by p_o for m=-1 when T_o=T_i=P_i=0

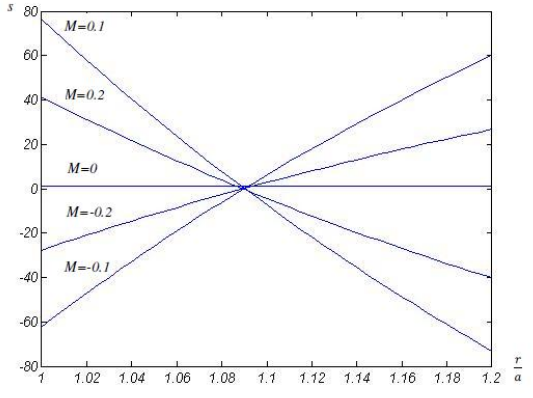

Figure (19-b) Effective mechanical stress for half of cylinder goes to plastic region causes by p_o for m=-1 when T_o=T_i=P_i=0

5 Conclusions

In the present work, an attempt has been made to study the problem of general solution for the thermal and mechanical stresses in a linear plastic thick FGM hollow cylinder due to the two-dimensional axisymmetric steady-state loads. The method of solution is based on the direct method and uses power series, rather than the potential function method. The advantage of this method is its mathematical power to handle mathematical function for the thermal and mechanical linear plastic stresses boundary conditions.
The material properties and yield strength through the graded direction are assumed to be nonlinear with a power law distribution. Depending on applied boundary condition, by selecting the optimum value of m, desirable level of radial and circumferential stresses could be obtained in FGM cylinders with respect to those in homogenous ones. By setting m = 0 in every equation, radial and circumferential stresses expressions turned to homogenous ones which could approve the validity of formulations. We can find the critical temperature and pressure that are very important for designing.

Nomenclature

T : Temperature
ε_{rr}^{p} : Radial linear plastic strain
ε_{rr} : Elastic strain
σ_{rr} : Radial elastic stress
λ : Lame coefficient
ν : Poisson's ratio
α : Coefficient of thermal expansion
$\sigma_{\theta\theta}$: Circumferential stress
σ_{rr}^{p} : Radial linear plastic stress

References

[1] Lutz, M.P., and Zimmerman, R.W., "Thermal Stresses and Effective Thermal Expansion Coefficient of Functionally Graded Sphere", J. Therm. Stresses, Vol. 19, pp. 39-54, (1996).

[2] Zimmerman, R.W, and Lutz, M.P., "Thermal Stresses and Thermal Expansion in a Uniformly Heated Functionally Graded Cylinder", J. Therm. Stresses, Vol. 22, pp. 177-188, (1999).

[3] Jabbari, M., Sohrabpour, S., and Eslami, M.R., "General Solution for Mechanical and Thermal Stresses in Functionally Graded Hollow Cylinder Due to Radially Symmetric Loads", J. Appl. Mech. Vol. 70, pp. 111-118, (2003).

[4] Poultangari, R., Jabbari, M., and Eslami, M.R., "Functionally Graded Hollow Spheres under Non-axisymmetric Thermo-mechanical Loads", International Journal of Pressure Vessels and Piping, Vol. 85, pp. 295–305, (2008).

[5] Yunbing, L., Kayin, Zh., Jinsheng, X., and Dongsheng, W., "Thermal Stresses Analysis of Ceramic/metal Functionally Gradient Material Cylinder", Applied Mathematics and Mechanics, Vol. 20, No. 4, pp. 413-417, (2001).

[6] Shariyat, M., Lavasani, S.M.H., and Khaghani, M., "Transient Thermal Stress and Elastic Wave Propagation Analyses of Thick Temperature-dependent FGM Cylinders, using a Second-order Point-collocation Method", Appl. Math. Modell. Vol. doi:10.1016/j.apm. (2009.07.007).

[7] Shariyat, M., "A Nonlinear Hermitian Transfinite Element Method for Transient Behavior Analysis of Hollow Functionally Graded Cylinders with Temperature-dependent Materials under Thermo-mechanical Loads", International Journal of Pressure Vessels and Piping, Vol. 86, pp. 280–289, (2009).

[8] Lü, C.F., Chen, W.Q., and Lim, C.W., "Elastic Mechanical Behavior of Nano-scaled FGM Films Incorporating Surface Energies", Composites Science and Technology, Vol. 69, pp. 1124–1130, (2009).

[9] Li, X.Y., Ding, H.J., and Chen, W.Q., "Elasticity Solutions for a Transversely Isotropic Functionally Graded Circular Plate Subjectto an Axisymmetric Transverse Load QRK", International Journal of Solids and Structures, Vol. 45, pp. 191–210, (2008).

[10] Afsar, A.M., and Sekine, H., "Inverse Problems of Material Distributions for Prescribed Apparent Fracture Toughness in FGM Coatings around a Circular Hole in Infinite Elastic Media", Composites Science and Technology, Vol. 62, pp. 1063–1077, (2002).

[11] Tajeddini, V., Ohadi, A.R., and Sadighi, S., "Three-dimensional Free Vibration of Variable Thickness Thick Circular and Annular Isotropic and Functionally Graded Plates on Pasternak Foundation", International Journal of Mechanical Sciences, Vol. 53, pp. 300–308, (2011).

[12] Nosier, A., and Fallah, F., "Non-linear Analysis of Functionally Graded Circular Plates under Asymmetric Transverse Loading", International Journal of Nonlinear Mechanics, Vol. 44, pp. 928 – 942, (2009).

[13] Zhang, D-G., and Zhou, Y-H., "A Theoretical Analysis of FGM Thin Plates Based on Physical Neutral Surface", Computational Materials Science, Vol. 44, pp. 716–720, (2008).

[14] Fazelzadeh, S.A., and Hosseini, M., "Aerothermoelastic Behavior of Supersonic Rotating Thin-walledbeams Made of Functionally Graded Materials", Journal of Fluids and Structures, Vol. 23, pp. 1251–1264, (2007).

[15] Ootao, Y., and Tanigawa, Y., "Transient Thermoelastic Problem of Functionally Graded Thick Strip Due to Non Uniform Heat Supply", Compose Struct. Vol. 63, No. 2, pp. 139-146, (2004).

[16] Jabbari, M., Sohrabpour, S., and Eslami, M.R., "Mechanical and Thermal Stresses in a Functionally Graded Hollow Cylinder Due to Radially Symmetric Loads", International Journal of Pressure Vessels and Piping, Vol. 79, pp. 493–497, (2002).

[17] Farid, M., Zahedinejad, P., and Malekzadeh, P., "Three-dimensional Temperature Dependent Free Vibration Analysis of Functionally Graded Material Curved Panels Resting on Two-parameter Elastic Foundation using a Hybrid Semi-analytic, Differential Quadrature Method", Materials and Design, Vol. 31, pp. 2–13, (2010).

[18] Bagri, A., and Eslami, M.R., "Generalized Coupled Thermoelasticity of Functionally Graded Annular Disk Considering the Lord–Shulman Theory", Composite Structures. Vol. 83, pp. 168–179, May (2007).

[19] Samsam Shariat, B.A., and Eslami, M.R., "Buckling of Thick Functionally Graded Plates under Mechanical and Thermal Loads", Composite Structures, Vol. 78, pp. 433–439, (2007).

[20] Jabbari, M., Bahtui, A., and Eslami, M.R., "Axisymmetric Mechanical and Thermal Stresses in Thick Short Length Functionally Graded Material Cylinder", Int. J. pressure Vessels and Piping, Vol. 86, pp. 296-306, (2009).

[21] Zamani Nejad, M., and Rahimi, G.H., "Deformations and Stresses in Rotating FGM Pressurized Thick Hollow Cylinder under Thermal Load", Scientific Research and Essay Vol. 4, No. 3, pp. 131-140, March (2009).

[22] Batra, R.C., and Iaccarino, G.L., "Exact Solutions for Radial Deformations of a Functionally Graded Isotropic and Incompressible Second-order Elastic Cylinder", International Journal of Non-Linear Mechanics, Vol. 43, pp. 383-398, (2008).

[23] Shao, Z.S., and Wang, T.G., "Three-dimensional Solutions for the Stress Fields in Functionally Graded Cylindrical Panel with Finite Length and Subjected to Thermal/mechanical Loads", International Journal of Solids and Structures, Vol. 43, Issue. 13, pp. 3856-3874, (2006).

[24] Lubliner, J., "*Plasticity Theory*", Revised Edition, Pearson Education, (2006).

[25] Shabanaa, Y.M., and Noda, N., "Thermo-elasto-plastic Stresses in Functionally Graded Materials Subjected to Thermal Loading Taking Residual Stresses of the Fabrication Process into Consideration", Composites, Part B, Vol. 32, pp. 111-121, (2001).

[26] Eraslan, A.N., and Akis, T., "Plane Strain Analytical Solutions for a Functionally Graded Elastic–plastic Pressurized Tube", International Journal of Pressure Vessels and Piping, Vol. 83, No. 9, pp. 635-644, (2006).

[27] Eraslan, A.N., and Arslan, E., "Plane Strain Analytical Solutions to Rotating Partially Plastic Graded Hollow Shafts", Turkish J. Eng. Env. Sci. Vol. 31, pp. 273-288, (2007).

[28] Eraslan, A.N., and Akis, T., "Elastoplastic Response of a Long Functionally Graded Tube Subjected to Internal Pressure", Turkish J. Eng. Env. Sci. Vol. 29, pp. 361- 368, (2005).

[29] Nemat-Alla, M., Ahmed, K. I. E., and Allah, I. H., "Elastic–plastic Analysis of Two-dimensional Functionally Graded Materials under Thermal Loading", International Journal of Solids and Structures, Vol. 46, Issue. 14, pp. 2774-2786, (2009).

[30] Lu, H. Ç., "Stress Analysis in a Functionally Graded Disc under Mechanical Loads and a Steady State Temperature Distribution", Indian Academy of Sciences Sadhana, Vol. 36, Part 1, pp. 53–64, February (2011).

[31] Jahromi, B. H., "Elasto-plastic Stresses in a Functionally Graded Rotating Disk", Journal of Engineering Materials and Technology, Vol. 134, pp. 021004-021015, April (2012).

[32] Sadeghian, M., and Toussi, H. E., "Elasto-plastic Axisymmetric Thermal Stress Analysis of Functionally Graded Cylindrical Vessel", J. Basic. Appl. Sci. Res., Vol. 2, No. 10, pp. 10246-10257, (2012).

[33] Mendelson, A., "*Plasticity: Theory and Application*", New York, MacMillan, (1986).

Appendixes

Appendix A:

$$A_1=\frac{c_{21}f_1-c_{11}f_2}{c_{21}\left(-\frac{c_{11}a^{-m_3}}{m_3}+c_{12}a^{-(m_3+1)}\right)-c_{11}\left(-\frac{c_{21}b^{-m_3}}{m_3}+c_{22}b^{-(m_3+1)}\right)}$$

$$A_2=\frac{\left(-\frac{c_{11}a^{-m_3}}{m_3}+c_{12}a^{-(m_3+1)}\right)f_2-\left(-\frac{c_{21}b^{-m_3}}{m_3}+c_{22}b^{-(m_3+1)}\right)f_1}{c_{21}\left(-\frac{c_{11}a^{-m_3}}{m_3}+c_{12}a^{-(m_3+1)}\right)-c_{11}\left(-\frac{c_{21}b^{-m_3}}{m_3}+c_{22}b^{-(m_3+1)}\right)}$$

$$g_1=(3-m_1)$$

$$g_2=m_1(v-1)$$

$$g_3=\frac{(m_2\alpha_0E_0A_{1)}}{m_3}-\alpha_0E_0A_1$$

$$g_4=-m_2\alpha_0E_0A_2$$

$$g_5=E_0$$

$$g_6=2E_0$$

$$H_1=\frac{g_3}{(m_1+m_2-m_3)(m_1+m_2-m_3-1)+(m_1+m_2-m_3)g_1+g_2}$$

$$H_2=\frac{g_4}{(m_1+m_2)(m_1+m_2-1)+(m_1+m_2)g_1+g_2}$$

$$H_3 = \frac{g_5}{(m_1+1)m_1+(m_1+1)g_1+g_2}$$

$$H_4 = \frac{g_6}{m_1 g_1+g_2+(m_1-1)m_1}$$

$$I_1 = \frac{H_1(a^{z_2}b^{m_1+m_2-m_3}-b^{z_2}a^{m_1+m_2-m_3})+H_2(a^{z_2}b^{m_1+m_2}-b^{z_2}a^{m_1+m_2})+H_3(a^{z_2}\epsilon_{b,r}^{p}b^{m_1+1}-b^{z_2}\epsilon_{a,r}^{p}a^{m_1+1})}{a^{z_1}b^{z_2}-a^{z_2}b^{z_1}}+$$

$$\frac{H_4(a^{z_2}\epsilon_{b}^{p}b^{m_1}-b^{z_2}\epsilon_{a}^{p}a^{m_1})}{a^{z_1}b^{z_2}-a^{z_2}b^{z_1}}$$

$$I_2 = \frac{H_1(a^{z_2}b^{m_1+m_2-m_3}-b^{z_1}a^{m_1+m_2-m_3})+H_2(a^{z_1}b^{m_1+m_2}-b^{z_2}a^{m_1+m_2})+H_3(a^{z_1}\epsilon_{b,r}^{p}b^{m_1+1}-b^{z_1}\epsilon_{a,r}^{p}a^{m_1+1})}{a^{z_1}b^{z_2}-a^{z_2}b^{z_1}}+$$

$$\frac{H_4(a^{z_2}\epsilon_{b}^{p}b^{m_1}-b^{z_2}\epsilon_{a}^{p}a^{m_1})}{a^{z_1}b^{z_2}-a^{z_2}b^{z_1}}$$

Appendix B:

$$K_2 = \frac{-p_i b^{z_1}-H_3(\varepsilon_{a,r}^{p}a^{m_1+1}b^{z_1}-\varepsilon_{b,r}^{p}b^{m_1+1}a^{z_1})-H_4(\varepsilon_{a}^{p}a^{m_1}b^{z_1}-\varepsilon_{b}^{p}b^{m_1}a^{z_1})}{a^{z_2}b^{z_1}-b^{z_2}a^{z_1}}$$

$$K_1 = \frac{-p_i b^{z_2}-H_3(\varepsilon_{a,r}^{p}a^{m_1+1}b^{z_2}-\varepsilon_{b,r}^{p}b^{m_1+1}a^{z_2})-H_4(\varepsilon_{a}^{p}a^{m_1}b^{z_2}-\varepsilon_{b}^{p}b^{m_1}a^{z_2})}{a^{z_1}b^{z_2}-b^{z_1}a^{z_2}}$$

Appendix C:

$$A_3 = \frac{(1+\upsilon)(\mathrm{m}_1+\mathrm{m}_2)\alpha_0 A_2}{(1-\upsilon)}$$

$$A_4 = \frac{(1+\upsilon)\left(1-\frac{\mathrm{m}_1+\mathrm{m}_2}{\mathrm{m}_3}\right)\alpha_0 A_1}{(1-\upsilon)}$$

$$\eta_1 = \frac{-m_1}{2}+\left(\frac{-m_1}{4}^{2}-\frac{m_1\upsilon}{(1-\upsilon)}+1\right)^{0.5}$$

$$\eta_2 = \frac{-m_1}{2} - \left(\frac{-m_1}{4}^2 - \frac{m_1\upsilon}{(1-\upsilon)} + 1\right)^{0.5}$$

$$D_1 = \frac{A_3}{m_2(m_2+1) + (m_1+1)(m_2+1) + \left(\frac{m_1\upsilon}{(1-\upsilon)} - 1\right)}$$

$$D_2 = \frac{A_4}{(m_2-m_3)(m_2-m_3+1) + (m_1+1)(m_2-m_3+1) + \left(\frac{m_1\upsilon}{(1-\upsilon)} - 1\right)}$$

$$d_1 = ((1-v)\eta_1 + v)\,a^{m_1+\eta_1-1}$$

$$d_2 = ((1-v)\eta_2 + v)\,a^{m_1+\eta_2-1}$$

$$d_3 = ((1-v)\eta_1 + v)\,b^{m_1+\eta_1-1}$$

$$d_4 = ((1-v)\eta_2 + v)\,b^{m_1+\eta_2-1}$$

These two constants of integration (d_5, d_6) are for thermal stresses

$$d_5 = -(((1-v)m_2+1)D_1 - (1-v)\alpha_0 A_2)\,a^{m_1+m_2} - (((1-v)(m_2-m_3)+1)D_2 + \frac{(1+v)\alpha_0 A_2}{m_3})a^{m_1+m_2-m_3}$$

$$d_6 = -(((1-v)m_2+1)D_1 - (1-v)\alpha_0 A_2)\,a^{m_1+m_2} - (((1-v)(m_2-m_3)+1)D_2 + \frac{(1+v)\alpha_0 A_1}{m_3})a^{m_1+m_2-m_3}$$

These two constants of integration (d_5, d_6) are for mechanical stresses

$$d_5 = -(1+v)(1-2v)\frac{p_i}{E_i}$$

$$d_6 = 0$$

$$B_1 = \frac{d_4 d_5 - d_2 d_6}{d_4 d_1 - d_2 d_3}$$

$$B_2 = \frac{d_3 d_5 - d_1 d_6}{d_3 d_2 - d_1 d_4}$$

Appendix D:

$$A_5=\frac{(1+v)(\mathrm{m}_1+\mathrm{m}_2)\alpha_0\left(\frac{-c_{11}a^{-m_3}}{m_3}+c_{12}a^{-(m_3+1)}\right)}{(1-\mathrm{v})\left[\mathrm{c}_{21}\left(\frac{-c_{11}a^{-m_3}}{m_3}+c_{12}a^{-(m_3+1)}\right)-c_{11}\left(\frac{-c_{21}b^{-m_3}}{m_3}+c_{22}b^{-(m_3+1)}\right)\right]}$$

$$A_6=\frac{(1+v)(\mathrm{m}_1+\mathrm{m}_2)\alpha_0\left(\frac{-c_{11}b^{-m_3}}{m_3}+c_{12}b^{-(m_3+1)}\right)}{(1-\mathrm{v})\left[\mathrm{c}_{21}\left(\frac{-c_{11}a^{-m_3}}{m_3}+c_{12}a^{-(m_3+1)}\right)-c_{11}\left(\frac{-c_{21}b^{-m_3}}{m_3}+c_{22}b^{-(m_3+1)}\right)\right]}$$

$$A_3=A_5f_2+A_6f$$

$$A_7=\frac{(1+\upsilon)\left(1-\frac{\mathrm{m}_1+\mathrm{m}_2}{\mathrm{m}_3}\right)\alpha_0}{(1-\upsilon)\left[\,c_{21}\left(-\frac{c_{11}a^{-m_3}}{m_3}+c_{12}a^{-(m_3+1)}\right)-c_{11}\left(-\frac{c_{21}b^{-m_3}}{m_3}+c_{22}b^{-(m_3+1)}\right)\right.}$$

$$A_4=A_7\left(f_1-f_2\right)$$

$$A_8=\frac{A_5}{\mathrm{m}_2\left(\mathrm{m}_2+1\right)+\left(\mathrm{m}_1+1\right)\left(\mathrm{m}_2+1\right)+\left(\frac{m_1\upsilon}{(1-\upsilon)}-1\right)}$$

$$A_9=\frac{A_6}{\mathrm{m}_2\left(\mathrm{m}_2+1\right)+\left(\mathrm{m}_1+1\right)\left(\mathrm{m}_2+1\right)+\left(\frac{m_1\upsilon}{(1-\upsilon)}-1\right)}$$

$$A_{10}=\frac{A_7}{\left(\mathrm{m}_2-\mathrm{m}_3\right)\left(\mathrm{m}_2-\mathrm{m}_3+1\right)+\left(\mathrm{m}_1+1\right)\left(\mathrm{m}_2-\mathrm{m}_3+1\right)+\left(\frac{m_1\upsilon}{(1-\upsilon)}-1\right)}$$

$$A_{11}=\frac{\left(-\frac{c_{11}a^{-m_3}}{m_3}+c_{12}a^{-(m_3+1)}\right)}{\left[c_{21}\left(-\frac{c_{11}a^{-m_3}}{m_3}+c_{12}a^{-(m_3+1)}\right)-c_{11}\left(-\frac{c_{21}b^{-m_3}}{m_3}+c_{22}b^{-(m_3+1)}\right)\right]}$$

$$A_{12}=\frac{\left(-\frac{c_{11}b^{-m_3}}{m_3}+c_{12}b^{-(m_3+1)}\right)}{\left[c_{21}\left(-\frac{c_{11}a^{-m_3}}{m_3}+c_{12}a^{-(m_3+1)}\right)-c_{11}\left(-\frac{c_{21}b^{-m_3}}{m_3}+c_{22}b^{-(m_3+1)}\right)\right]}$$

$$A_2 = A_{13}\left(f_1 - f_2\right)$$

$$A_{13} = \frac{1}{\left[c_{21}\left(-\frac{c_{11}a^{-m_3}}{m_3} + c_{12}a^{-(m_3+1)}\right) - c_{11}\left(-\frac{c_{21}b^{-m_3}}{m_3} + c_{22}b^{-(m_3+1)}\right)\right]}$$

$$A_1 = A_{13}\left(f_1 - f_2\right)$$

$$d_7 = -((1-v)m_2 + 1)a^{m_1+m_2}$$

$$d_8 = -(1+v)\alpha_0 a^{m_1+m_2}$$

$$d_9 = -((1-v)(m_2 - \mathrm{m}_3) + 1)a^{m_1+m_2-m_3}$$

$$d_{10} = -\left(\frac{(1+\upsilon)\alpha_0}{m_3}\right)a^{m_1+m_2-m_3}$$

$$d_{11} = -((1-v)m_2 + 1)b^{m_1+m_2}$$

$$d_{12} = -(1+v)\alpha_0 b^{m_1+m_2}$$

$$d_{13} = -((1-v)(m_2 - \mathrm{m}_3) + 1)b^{m_1+m_2-m_3}$$

$$d_{14} = -\left(\frac{(1+\upsilon)\alpha_0}{m_3}\right)b^{m_1+m_2-m_3}$$

$$d_5 = d_{15}f_2 + d_{16}f_1$$

$$d_6 = d_{17}f_2 + d_{18}f_1$$

$$d_{15} = (d_7A_8 + d_8A_{11} - d_9A_{10} - d_{10}A_{13})$$

$$d_{16} = (d_7A_9 + d_8A_{12} + d_9A_{10} + d_{10}A_{13})$$

$$d_{17} = (d_{11}A_8 + d_{12}A_{11} - d_{13}A_{10} - d_{14}A_{13})$$

$$d_{18} = (d_{11}A_9 + d_{12}A_{12} + d_{13}A_{10} + d_{14}A_{13})$$

$$\mathrm{d}_{19} = d_1d_4 - d_2d_3$$

$$d_{27} = \frac{d_4d_{16} - d_2d_{18}}{d_{19}}$$

$$d_{26} = \frac{d_4d_{15} - d_2d_{17}}{d_{19}}$$

$$d_{20} = \frac{d_1 d_{17} - d_3 d_{15}}{d_{19}}$$

$$d_{21} = \frac{d_1 d_{18} - d_3 d_{16}}{d_{19}}$$

$$d_{22} = \frac{E_0 \left(1 - \eta_1\right)}{\left(1 + v\right)}$$

$$d_{23} = \frac{E_0 \left(1 - \eta_2\right)}{\left(1 + v\right)}$$

$$d_{24} = \frac{-E_0 m_2}{\left(1 + v\right)}$$

$$d_{25} = \frac{-E_0 \left(m_2 - m_3\right)}{\left(1 + v\right)}$$

$$D_1 = d_8 f_2 + A_9 f_1$$

$$D_2 = A_{10} \left(f_1 - f_2\right)$$

$$B_1 = d_{26} f_2 + A_{27} f_1$$

$$B_2 = d_{20} f_2 + d_{21} f_1$$

چکیده

در این طرح عمومی تنش‌های حرارتی و مکانیکی متقارن و دو بعدی در یک استوانه‌ی توخالی با ضخامت کم و ساخته شده از مواد FGM ارائه می‌شود. شکل کلی شرایط مرزی، در سطح داخل و خارج بررسی شده است. یک روش مستقیم برای حل دستگاه غیر همگن معادلات دیفرانسیلی ناویر با استفاده از حل عمومی و خصوصی و سری فوریه‌ی مختلط و روش تابع قانون توان به کار رفته است. خواص مواد به جز نرخ پوآسون وابسته به متغیر شعاع r فرض شده و به صورت تابع قانون توان نشان داده شده‌اند. نتایج، مقایسه‌ی نمودارها و تنش‌ها را نشان می‌دهد. ازآنجایی که مواد ناهمگن غالباً به دو دسته تقسیم بندی می شوند که یک دسته مواد چند ماده‌ای است که دارای چند فاز متمایز مادی است و دسته دیگر مواد با خصوصیات متغیر که درصد ماده تشکیل دهنده آن‌ها از نقطه ای به نقطه دیگر به صورت تابع پیوسته تغییر می کند.

این دسته در واقع کلاس جدیدی از مواد مرکب هستند که خصوصیات مواد در آنها در طول جسم، به صورت پیوسته تغییر می کند. مواد هدفمند در واقع ترکیبی از دو یا چند فاز مادی است و به گونه ای طراحی شده است که نسبت حجمی آن‌ها در یک یا چند جهت تغییر نماید. این عامل جسم مادی را از دیدگاه میکروسکوپی ناهمگن می‌سازد و از دیدگاه ماکروسکوپی خواص مکانیکی را به نرمی و به طور پیوسته تغییر می‌دهد. روش‌هایی برای حل معادلات این دسته از مواد وجود دارند که از جمله می توان استفاده از سری توانی، روش چند لایه‌ای، روش اختلالات، روش‌های المان محدود با در نظر گرفتن خواص ماده هدفمند با یک تابع مشخص (مانند تابع نمایی و...) را نام برد.